Chapter 5

3D Digital Simulation for Material Damage Mechanism Identification in a Railway Carriage Pressure Vessel

Alessandra Caggiano and Roberto Teti

Additional information is available at the end of the chapter

http://dx.doi.org/10.5772/intechopen.73233

Abstract

Digital simulation approaches applied to railway engineering allow to investigate different railway scenarios via 3D digital twins of real objects, motion simulation, and collision detection to identify the root causes of critical damage and estimate the most likely sources of railway accidents. In this work, a digital simulation approach is applied to a real catastrophic train accident in which a railway carriage carrying a pressure vessel collided with an obstacle that generated a cut in the pressure vessel casing. This cut initiated a liquefied petroleum gas leakage that expanded in the environment and caused the explosion and blaze responsible for human casualties. Traditional railway accident reconstruction procedures identified two potential objects accountable for the cutting of the pressure vessel casing: a wing rail and a track reference stake. Based on digital terrain models and reconstructed models of the railway carriage, 3D digital simulation scenarios were created to detect every possible collision of the pressure vessel with the infrastructure environment and investigate whether the shape of the cut in the pressure vessel wall fits the damage visible on the obstacles and whether the interference between obstacle and pressure vessel wall could generate the chip through an interaction similar to metal cutting.

Keywords: railway carriage, pressure vessel, safety, material damage, catastrophic accident, digital twin

1. Introduction

The employment of digital simulation approaches in railway engineering enables to explore various railway scenarios through the use of 3D digital twins of real objects, motion simulation, and collision detection, which represent valuable tools to detect the original causes of critical damage and estimate the most liable sources of railway accidents.

In a real catastrophic train accident, a railway carriage carrying a pressure vessel collided with an obstacle that generated a cut in the casing of the pressure vessel, initiating a liquefied petroleum gas leakage that expanded in the environment and caused the explosion and fire responsible for a high number of human casualties.

The utilization of traditional railway accident reconstruction procedures allowed to recognize two objects potentially accountable for the cutting of the pressure vessel casing: a wing rail and a track reference stake. In this work, based on digital terrain models and reconstructed models of the railway carriage obtained via reverse engineering, different 3D digital simulation scenarios are created, allowing to move and rotate the carriage interactively, as well as to examine the accident scene from different points of view, with the aim to detect every possible collision of the pressure vessel with the infrastructure environment. The scope of the 3D digital simulation employment is to investigate whether the form of the cut in the pressure vessel wall fits to the damage visible on the two potential objects accountable for the cutting of the pressure vessel casing and whether the interference between object and pressure vessel wall could generate the chip through an interaction similar to metal cutting.

2. Catastrophic train accident description and reconstruction

On the 29th of June 2009, around midnight, a catastrophic train accident occurred in the train station of Viareggio, Italy [1]. The train was a freight train with 14 carriages carrying pressure vessels filled with liquefied petroleum gas. After the accident, the whole train divided up into five separated parts: part 1 was the locomotive, still upright on the rails; part 2 was carriage no. 1, reversed on its left side; part 3 consisted of 2 carriages, nos. 2 and 3, still connected to each other and reversed on their left side; part 4 consisted of 2 carriages, nos. 4 and 5, still connected to one another and reversed on their left side; and part 5 was subdivided into two halves: the first half of part 5 consisted of five carriages, from carriage no. 6 to carriage no. 10, connected to each other and derailed but not reversed. The second half of part 5 consisted of four carriages, from carriage no. 11 to carriage no. 14, connected to each other and upright on the rails.

Each carriage carrying a pressure vessel had a front bogie and a back bogie; each bogie had a first (front) axle and a second (rear) axle [2–4].

The train derailment was caused by the sudden failure of the second axle of the front bogie of carriage number 1 [5, 6]. The axle breakage was caused by rotating flexural fatigue, determining a fatigue crack extension up to more than 65% of the axle resisting section. **Figure 1** [6] shows that the axle was fractured externally with respect to the left wheel (**Figure 1a**), and this failure was the original cause of the train derailment. **Figure 1b** illustrates the characteristic fatigue failure of the fracture surface of the axle on the wheel side: presence of a smooth area related to the slow propagation of the fatigue crack (upper zone in the image) and of a rough area of rapid failure of the residual axle section (lower zone in the image). The same characteristic fatigue failure is observable on the matching axle fracture surface on the axle box side.

http://dx.doi.org/10.5772/intechopen.73233

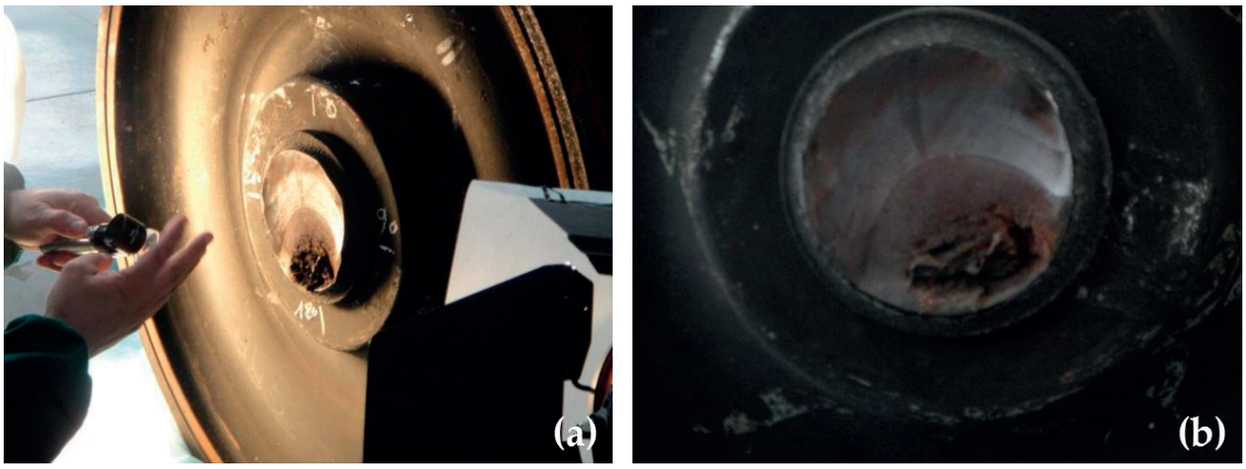

Figure 1. (a) Fatigue failure of the fracture surface of the axle on the wheel side. (b) Presence of a smooth area related to the slow propagation of the fatigue crack and of a rougher area of rapid failure of the residual axle section.

As regards the right wheel of the second wheelset (rear) of the front bogie of carriage no. 1, the right extremity of the axle did not break, but clear signs of corrosion are evidenced at the fillet between the axle extremity, called axel spindle, with a smaller diameter, and the axle zone with a larger diameter for shrink fitting of the wheel.

Figure 2 shows the bogie model Y25 mounted on the pressure vessel carriages composing train no. 50325, with indication of some of its components, including the axle boxes. Due to a fatigue crack in its final development phase transversally with respect to the wheelset axle, the vertical rigidity of the axle box supported by the axel spindle was notably reduced up to reaching a nonequilibrium condition of the vertical forces pressing the wheels on the rails. The surmounting of the rail occurred due to a notable reduction of the vertical force acting on the right front wheel, diagonally opposed to the force acting on the weakened axle spindle (left rear wheel).

Under these conditions, the transversal (horizontal) force acting on the right front wheel, which was no longer loaded downward by a sufficient vertical force, was high enough to

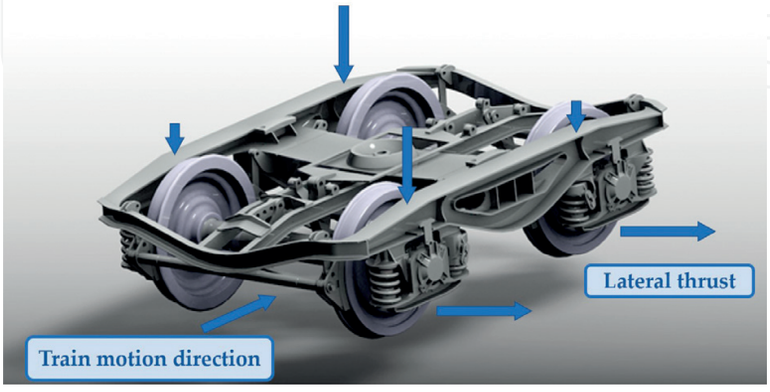

Figure 2. Forces acting on the first bogie of carriage no. 1 after breakage of the second axle (rear wheelset) due to fatigue failure externally with respect to the left wheel.

make the wheel climb over the top of the rail, causing the derailment of the front wheelset of the first bogie of carriage no. 1. The derailment start was located at km 120 + 265, next to Viareggio station entry when coming from the north (from Genoa station).

Figure 3 shows the traces of the initial phase of the derailment and in particular: (a) the start of the surmounting of the rail by the right front wheel of the first bogie of carriage no. 1. (b) The sleepers cut by the left wheel and the sidewalk curb abraded by the right front axle box of the first bogie of carriage no. 1.

Figure 4 shows the relative positions, after the derailment, of carriage no. 1, the rotated front bogie, the right front axle box abrading the sidewalk curb, and the abraded sidewalk curb. The derailed bogie rotated around its axis in clockwise direction with respect to the vertical axis in a reference system consistent with the train.

Near the end of the sidewalk, in the southward direction (toward Pisa station), there is a walkway at grade endowed with a slanted ramp (**Figure 5**). Until the walkway at grade, the derailed carriage had been guided by the sidewalk curb that acted on the highly abraded right front axle box just like a grinding wheel on a workpiece in a grinding process.

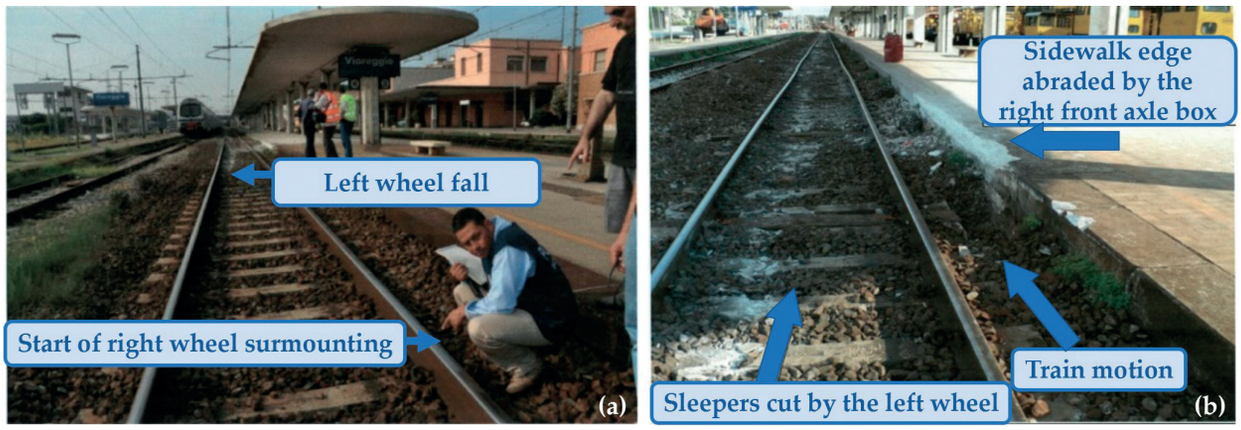

Figure 3. Traces of the initial phase of the derailment. (a) Start of the surmounting of the rail by the right front wheel of the first bogie of carriage no. 1. (b) Sleepers cut by the left wheel and sidewalk edge abraded by the right front axle box of the first bogie of carriage no. 1.

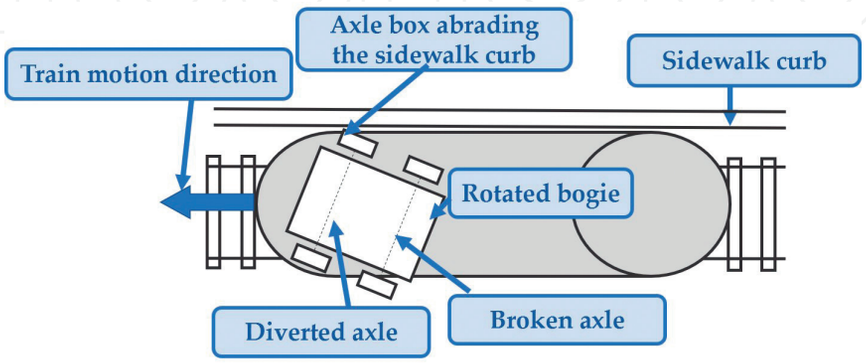

Figure 4. Relative positions, after derailment, of carriage no. 1, right front axle box, and sidewalk curb.

http://dx.doi.org/10.5772/intechopen.73233

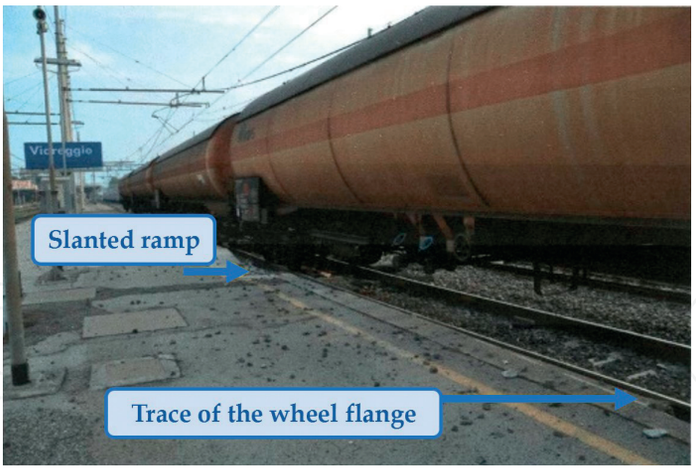

Figure 5. Walkway at grade endowed with a slanted ramp on the sidewalk, near the track of the derailed train, and trace on the granite curb left by the flange of the right wheel of the front wheelset of the first bogie of carriage no. 1.

Upon arriving at the slanted ramp of the walkway at grade, the front bogie of carriage no. 1, deprived of the guide provided on its right by the curb of the sidewalk and still pulled by the locomotive, engaged the slanted ramp with the right wheel of the first wheelset, climbing on the sidewalk and leaving on it the trace of the wheel flange as shown in **Figure 5**.

The upward movement of the carriage due to the climbing provoked its overturning on its left side in the train motion direction, as described below.

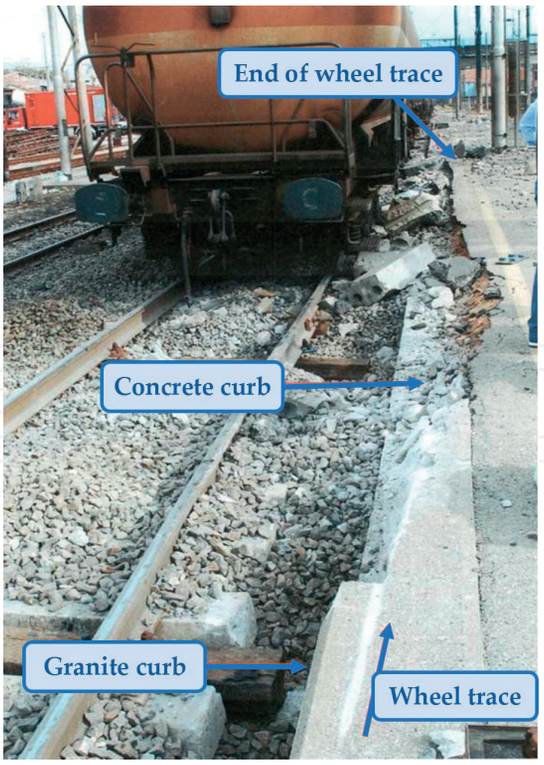

Figure 6. Concrete sidewalk damaged by the right wheel of the front wheelset of the first bogie of carriage no. 1 and starting point of the carriage overturning.

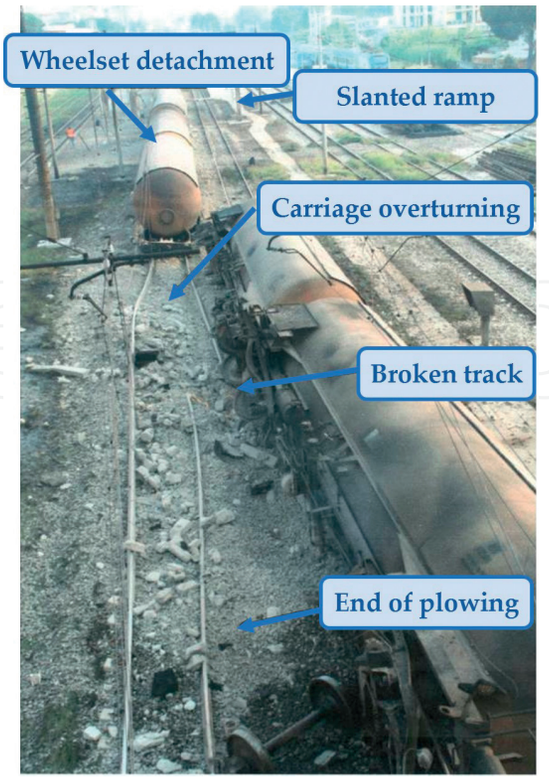

Figure 7. Superstructure zone wrecked due to the "plowing" mechanism of the track by the front wheelset of the first bogie.

Few meters after the end of the walkway at grade, the curb material, made of granite up to that point, changed into a concrete structure that completely crumbled under the action of the wheel due to much lower strength of the concrete material (see **Figure 6**).

At the end of the concrete sidewalk zone, crumbled by the right wheel of the front wheelset of the first bogie, the overturning of carriage no. 1 on its left side in the train motion direction started. The carriage continued its course till it landed at about 73 m from the point where its detachment from the track began. The landing point of carriage no. 1 corresponds to the

Figure 8. Plowing mechanism of the track by the bogie of the overturned carriage.

http://dx.doi.org/10.5772/intechopen.73233

beginning of the superstructure zone wrecked by the "plowing" mechanism of the track, as shown in **Figure 7**.

When, at the end of the overturning phase, carriage no. 1 crashed onto the infrastructure, it presented the remaining wheelset still mounted on its first bogie with its axis slightly slanted forward and the wheel, originally on the left side in the train motion direction, stuck under the sleepers; as the carriage proceeded its course under these conditions, the track was plowed according to the mechanism illustrated in **Figure 8**.

After the end of the plowing zone, the carriage continued to slide on its left side along the railway superstructure.

3. Cut on the tank shell of carriage no. 1 and elements potentially responsible for the opening of the cut

In the final phase of the accident, shortly before carriage no. 1 finally ended its course, an external body present on the railway superstructure hit the pressure vessel and opened the cut on the tank shell shown in **Figure 9**.

From this cut, the liquefied petroleum gas came out in liquid phase under pressure and started the liquid-gas phase transformation, creating a gaseous cloud that expanded in the environment. After about 190 s, accidental causes determined the ignition of the gaseous cloud and the catastrophic consequences of the accident.

Figure 10 shows the aerial view of the accident scenario with indication of the potentially responsible elements that could have generated the cut on the tank shell through a mechanism similar to the action of a metal cutting tool. The positions of the elements are reported in more details in **Figure 11**.

- Track reference stake no. 23, found under the pressure vessel at about 7 m from the back bumper of carriage no. 1.

Figure 9. Carriage no. 1 with a cut opening on the tank shell.

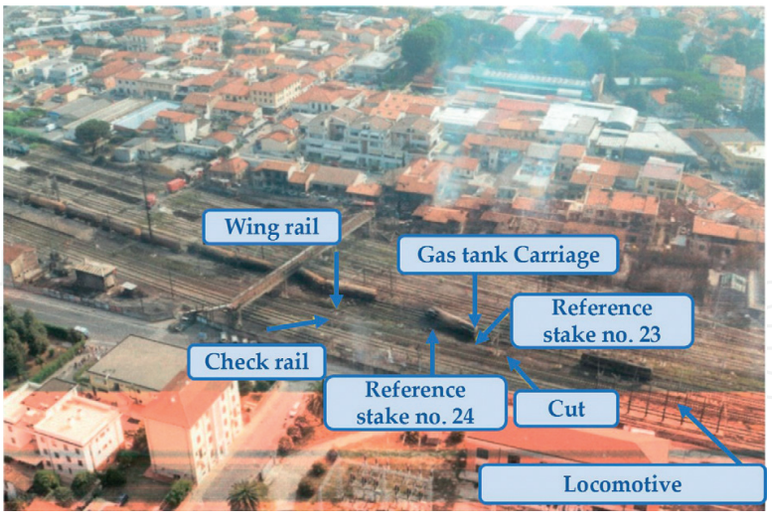

Figure 10. Aerial view of the accident with indication of the elements potentially responsible for the opening of the cut on the tank shell.

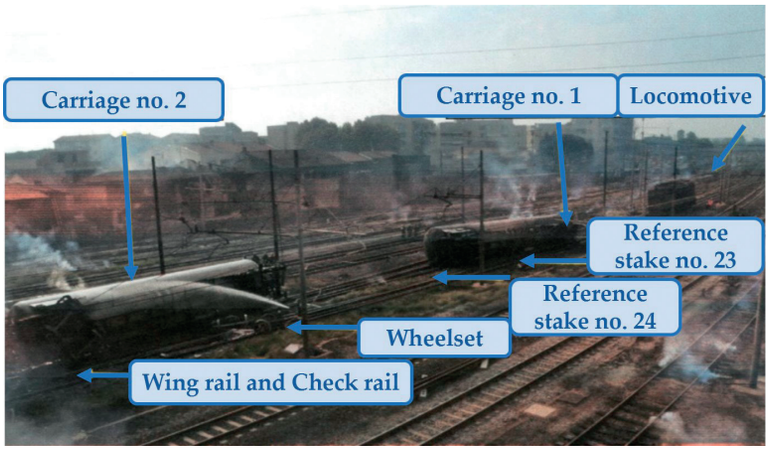

Figure 11. Positions of the elements potentially responsible for the cut generation on the tank shell through an action similar to metal cutting: track reference stake nos. 23 and 24, wing rail and check rail.

- Track reference stake no. 24, found at about 3 m before the back bumper of carriage no. 1.
- Wing rail and check rail [2–4] that may have been hit by diverse components of the rolling stock.

3.1. Track reference stake nos. 23 and 24

It is worth mentioning that a track curve reference stake is made of a chunk of rail anchored in a concrete plinth grounded in the ballast so that the reference stake protrudes vertically out of the ground level with an elevation 5 cm higher than the highest rail of the track curve. The function of the track reference stakes is to allow for the periodical checking of the correct geometry of the track curve next to which they are installed. To perform this checking, a technician periodically controls that the internal edge of the highest rail of the

http://dx.doi.org/10.5772/intechopen.73233

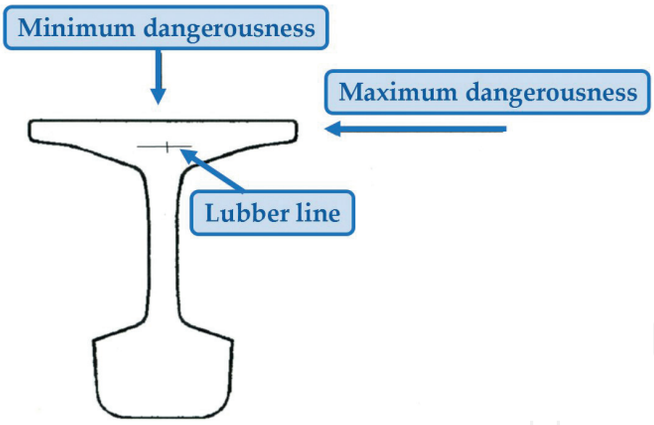

Figure 12. Transverse section of a track curve reference stake and directions of minimum and maximum danger grade in case of impact by a moving body against the track reference stake.

track curve is 1.5 m distant from the reference line traced on the top section of the track reference stake.

In **Figure 12**, the transverse section of a track curve reference stake is shown illustrating the variation of the degree of danger as a function of the impact direction of a moving body against the track reference stake. In the figure, two possible impact directions are considered: the one of maximum degree of danger, parallel to the lower surface of the rail chunk and the other of minimum degree of danger, perpendicular to the lower surface of the rail chunk. For intermediate impact angles, the danger increases going from a perpendicular impact to a parallel impact with reference to the lower surface of the rail chunk. In the latter case, the extremely high contact forces due to the sharp configuration of the corner of the lower surface of the rail chunk can easily determine the cutting of the sheet metal of the impacting tank shell.

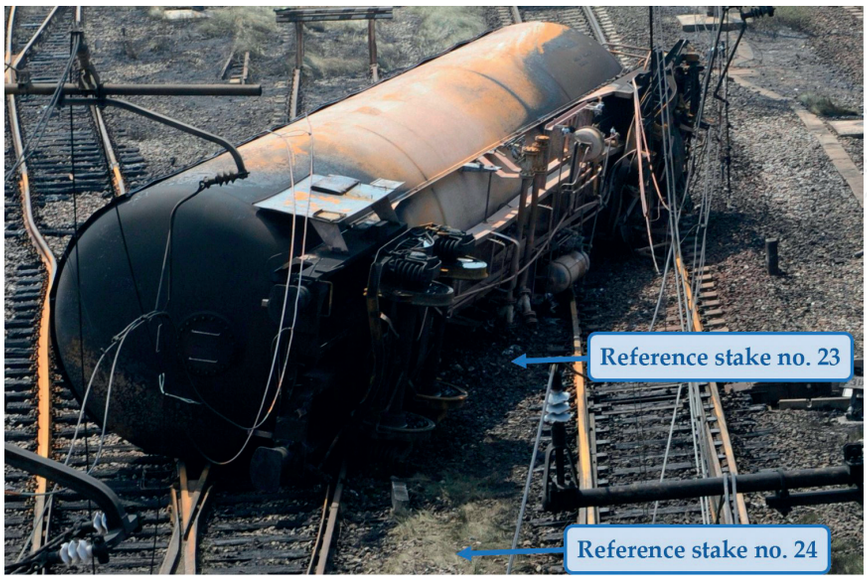

Figure 13. Rear view of carriage no. 1 in the accident scene and positions of track reference stake nos. 23 and 24.

Figure 13 shows the rear view of carriage no. 1 in the accident scene and the positions of track reference stake nos. 23 and 24; the two track reference stakes are 10 m apart, as set by the technical regulations of the Italian railways.

Figure 14 shows the front view of carriage no. 1 where it can be seen that the front bumper lies on the right rail in the train motion direction of track no. 4.

In **Figure 15**, a detail of track reference stake no. 24, found under the tank of carriage no. 1 almost completely buried in the track ballast, is shown. The sharp corner of the lower surface of the rail chunk, making up the track reference stake, appears highly abraded with its abraded metal surface still not subjected to oxidization. This confirms that the abrasion process, due to sliding against the carriage, was very recent during the examinations carried out in the accident scenario.

Figure 14. Front view of carriage no. 1 in the accident scene and position of its front bumper.

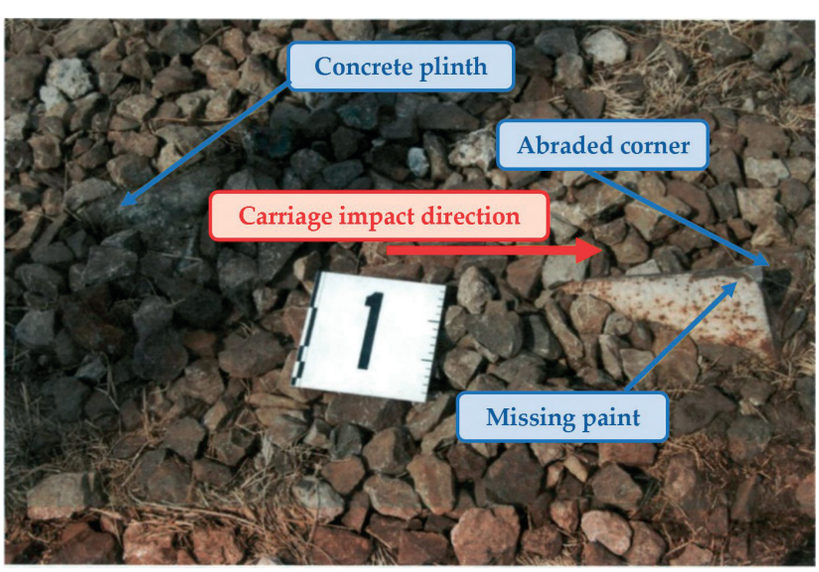

Figure 15. Track reference stake no. 24, photographed during the investigations on the accident site conditions, almost completely buried in the track ballast following its impact against the pressure vessel of carriage no. 1.

http://dx.doi.org/10.5772/intechopen.73233

Figure 16 shows track reference stake no. 24 after its extraction from the ballast: there are no traces of flexural deformation evidencing that the track reference stake had been solely rotated in a rigid way on its plinth during its knocking down under the impact action of the pressure vessel of carriage no. 1. Moreover, the figure shows the notable extension of the abrasion of the sharp corner of the lower surface of the track reference stake [6].

In **Figure 17**, a detail of track reference stake no. 23 knocked down by the pressure vessel of carriage no. 1 about 10 m after track reference stake no. 24 had been hit is shown. The track reference stake no. 23 was found under the tank, and its sharp corners did not show significant traces of abrasion. At the moment of impact against track reference stake no. 23, the carriage was by then almost steady and therefore endowed with a much lower kinetic energy with respect to the moment of impact against track reference stake no. 24.

3.2. Wing rail and check rail

Figure 18 shows a detail of the deformation of the wing rail. The impact on the wing rail has a component in the transverse direction, oriented toward the left side in the train motion direction, and there are no traces of abrasion due to sliding on the deformed zone of the wing rail.

Figure 16. Track reference stake no. 24 photographed after its extraction from the track ballast. (a) In the foreground: flange of the track reference stake with damaged edge; in the background: view of the concrete plinth; and (b) and (c) details of the damaged edge.

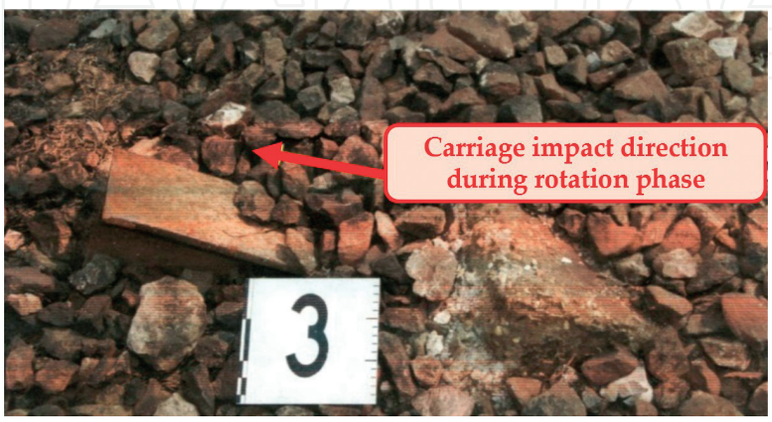

Figure 17. Track reference stake no. 23, photographed during the investigations on the accident site conditions, partially buried in the track ballast following its impact against the pressure vessel of carriage no. 1.

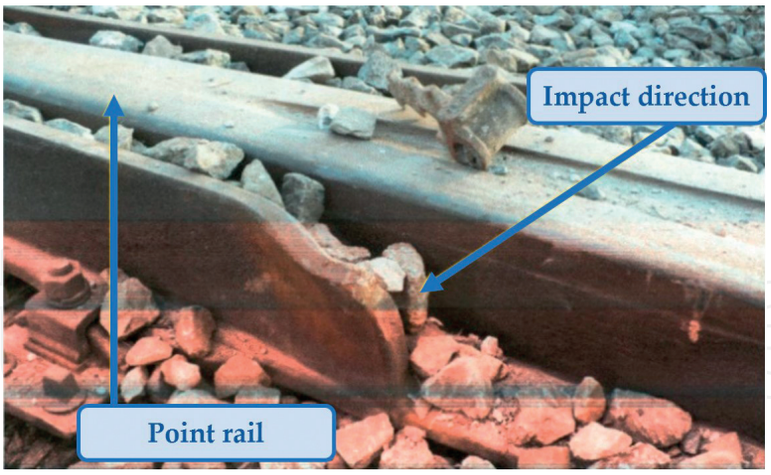

Figure 18. Wing rail photographed during the investigations at the accident site conditions.

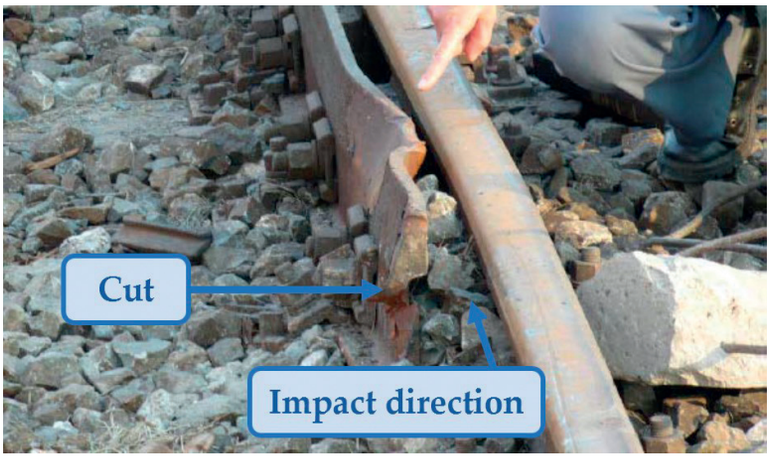

Figure 19. Check rail opposite to the wing rail photographed during the investigations on the accident site conditions.

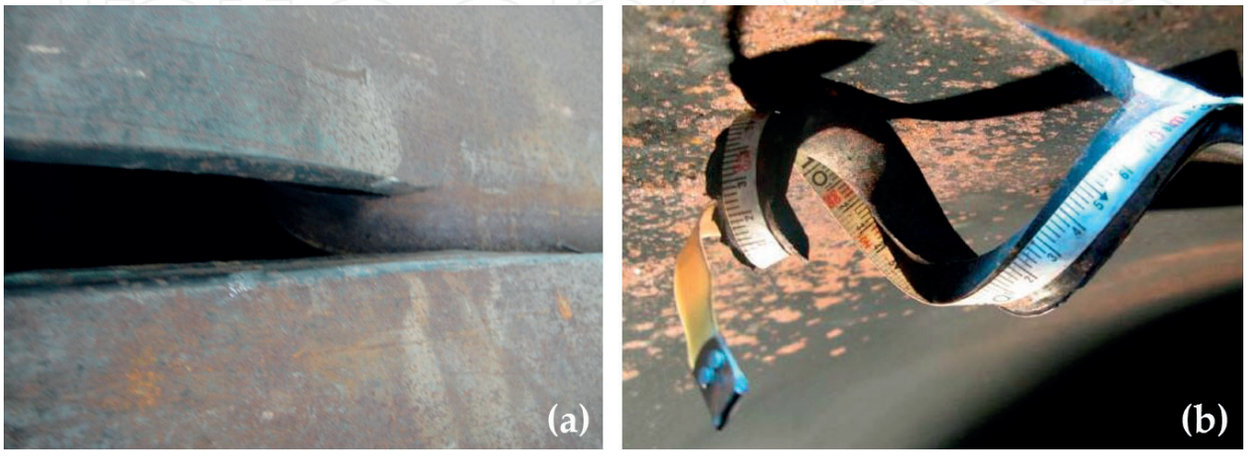

Figure 20. (a) Enlarged external view of the end side of the cut with the attached corresponding chip bent internally inside the tank shell and (b) enlarged internal view of the chip portion still attached to the tank shell.

http://dx.doi.org/10.5772/intechopen.73233

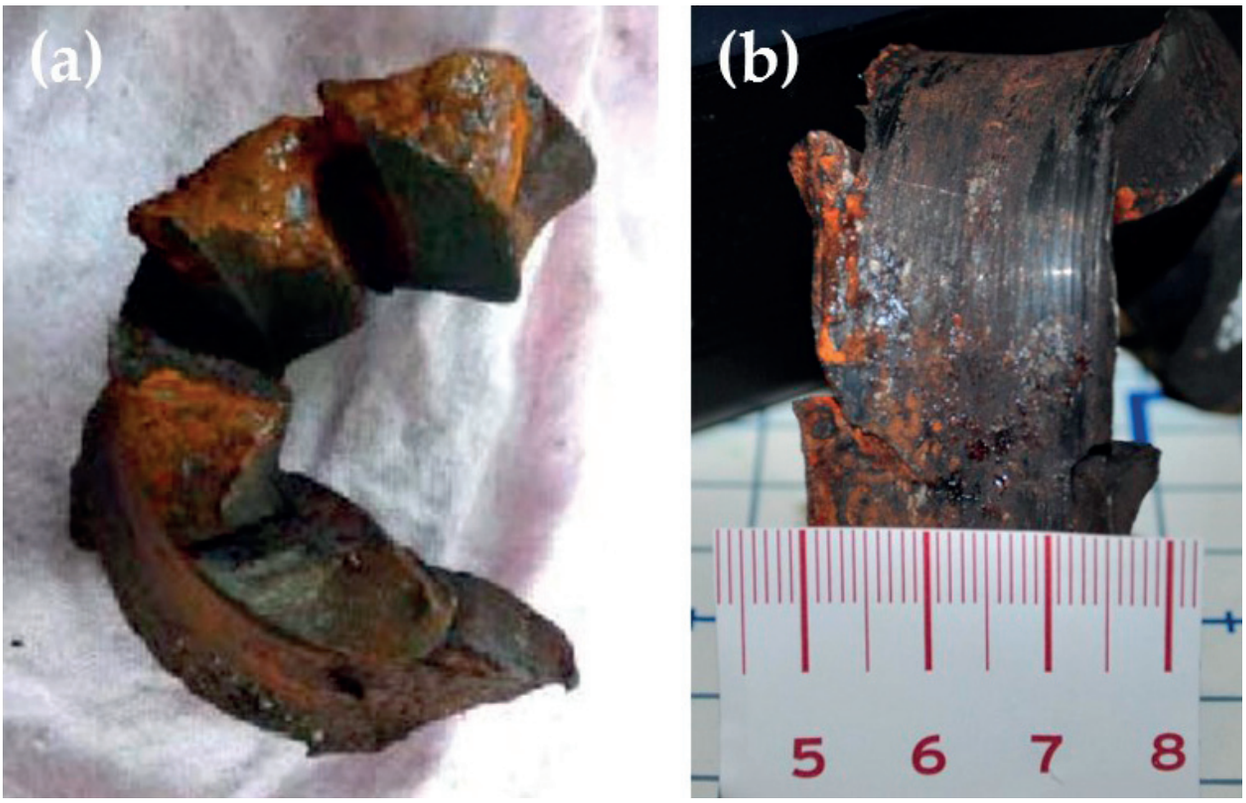

Figure 21. Chip portion detached from the tank shell showing the segmented morphology typical of a chip generated during a machining operation.

Figure 19 shows a detail of the deformation of the check rail opposite to the wing rail. It has been subject to a strong impact in the direction of motion of the overturned carriage no. 1. One element of the derailed material, sliding along the track, has hooked the check rail determining on it a cut and some bulges.

The final part of the chip remained attached to the tank shell (**Figure 20**), while the initial chip portion was detached from the shell and was found inside the tank. This segmented chip shows the typical morphology of a chip formed during a machining operation that generates a notable chip segmentation (**Figure 21**).

4. 3D Digital modeling and simulation analysis to identify the element responsible for the cut

To identify the element that generated the cut in the tank shell of carriage no. 1 through a mechanism similar to the action of a metal cutting tool, an approach based on 3D digital modeling and simulation was employed [7].

Digital simulation allows to investigate different scenarios through the use of 3D digital twins of real objects, motion simulation and detection of interferences, which are useful to identify the root causes of the critical cut damage on the tank shell.

Within the digital simulation scenarios, it was investigated whether the form of the cut in the pressure vessel fits to the damage found on the elements potentially accountable for the cutting of the tank shell and whether the interference between elements and tank shell could generate the chip through an interaction similar to metal cutting.

The 3D digital twins of the railway carriage and the elements potentially accountable for the cutting were obtained by acquiring the geometry and shape of the real parts and reconstructing their digital models via a reverse engineering (RE) procedure [8–10].

RE is the process of acquiring the geometry and shape of a part and reconstructing its digital model. The first stage of the RE procedure, i.e., digital data acquisition, can be carried out by means of several different tools [9, 11]. In this case, a time-of-flight laser sensor and a portable laser scanner with high accuracy were employed for scanning the railway carriage and the surrounding elements.

4.1. Track reference stake no. 23 exclusion and track reference stake no. 24 initial confirmation

In **Figure 22**, the directions of the impact between the tank of carriage no. 1 and track reference stake nos. 23 and 24 are evidenced. It is worth recalling that the tank first hit the track reference stake no. 24 and afterward the track reference stake no. 23.

During the interaction with track reference stake no. 24, which was hit first, the tank, under the action of the applied forces, initiated a rotational motion around a vertical axis, as endorsed by the arched shape of the cut on the tank shell.

Figure 23 illustrates the motion of tank carriage no. 1 when, after hitting track reference stake no. 24, it proceeded to hitting track reference stake no. 23. The rotation of the carriage around the vertical axis was about 5° clockwise for an observer looking at the scene from above.

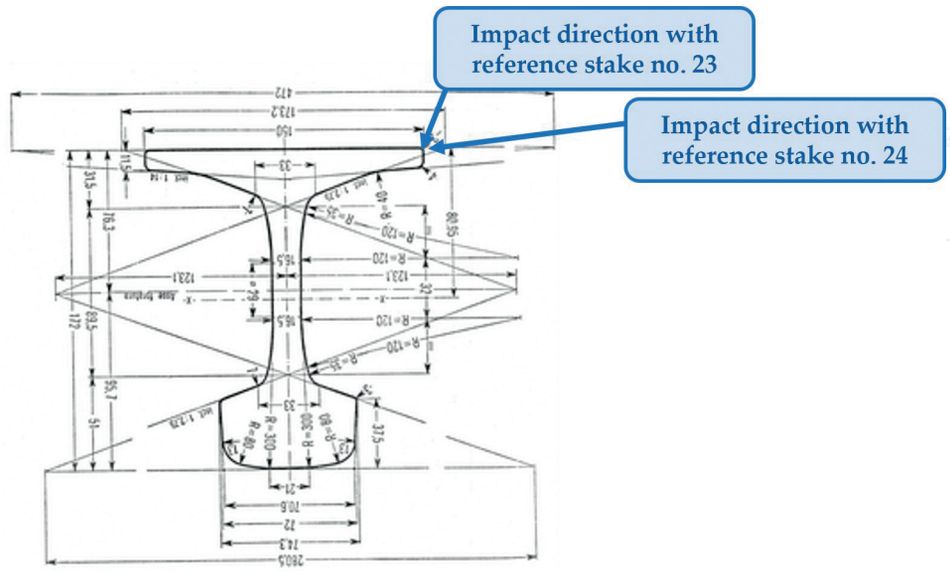

Figure 22. Direction of the impact between the tank of carriage no. 1 and track reference stake nos. 23 and 24.

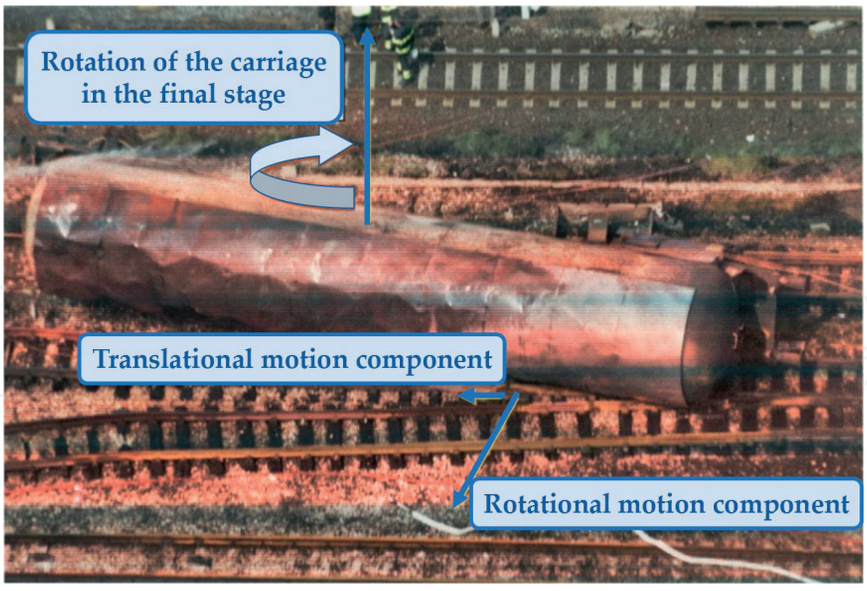

Figure 23. Rotational motion of tank carriage no. 1 around a vertical axis.

4.2. Check rail exclusion

Figure 24 shows a series of details of the core zone of railway switch 13B. The scene refers to the zone around the wing rail and the check rail as it appeared after the accident, where the following elements were found:

- The anchorage bracket of carriage no. 1, sitting at about 3.5 m beyond the position of the wing rail.
- A chunk of the right-side axle box, in the train motion direction, of the first (front) wheel set no. 85890 of the front bogie, i.e., the axle box which remained mounted on carriage no. 1 after the second (back) wheel set no. 98331 of the front bogie was detached.
- Part of the sheet metal billboard welded on the side of carriage no. 1 for the application of transport documentation.

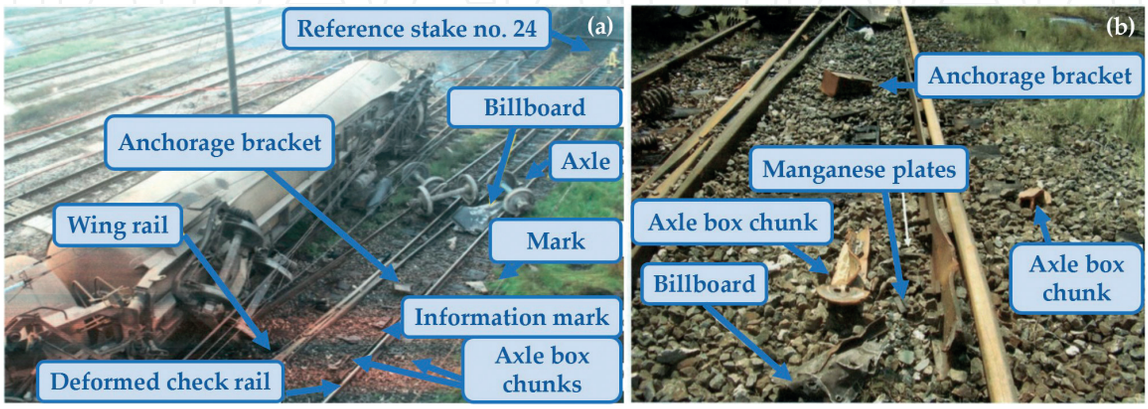

Figure 24. Zone of the heart of railway switch 13B around the wing rail and the check rail immediately after the accident.

- The manganese plates making up the kinematic surface on which the axle boxes slide with respect to the axel guard

All these wreckages demonstrate that the body, which strongly deformed the check rail, was an axle box that was practically destroyed during the impact (**Figure 25**).

Figure 26 shows two of the three chunks of the right axle box of the first wheelset of the front bogie of carriage no. 1, whereas **Figure 27** shows the digital model of the fragment of **Figure 26b** obtained by reverse engineering reconstruction based on geometry acquisition with a structured light optical sensor.

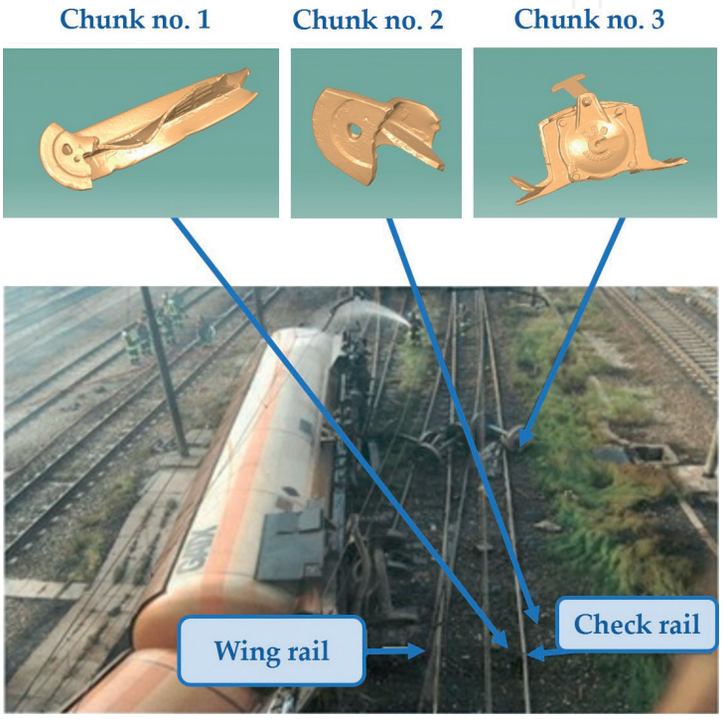

Figure 25. Position, in the accident scene, of the chunks of the right axle box of the front wheelset of the front boogie of carriage no. 1; the axle box was greatly abraded and broken into three fragments.

Figure 26. Two of the three chunks of the right axle box of the front wheel set of the front bogie of carriage no. 1: (a) chunk of the axle box found between the rails near the deformed check rail and (b) chunk of the axle box greatly abraded by the granite sidewalk curb exerting a grinding action on the right axle box, found externally to the track near the right-side rail in the train motion direction.

http://dx.doi.org/10.5772/intechopen.73233

Figure 27. Digital twin of the chunk of the right axel box of the first wheel set of the front bogey of carriage no. 1 obtained by reverse engineering reconstruction based on geometry acquisition with a structured light optical sensor.

The front part of the right axle box—right side in the train motion direction—of the front wheel set was greatly abraded by the granite of the sidewalk curb that acted on the right front axle box just like a grinding wheel on the workpiece in a grinding process (**Figures 26b** and **27**).

The realization of the digital twins of the check rail and the right axle box of the first wheel set of the front bogie of carriage no. 1, obtained by reverse engineering reconstruction based on geometry acquisition with a structured light optical sensor, allowed to reconstruct under simulation the kinematics of the impact between axle box and check rail, as illustrated in **Figure 28a**. **Figure 28b** shows the traces of damage on the check rail, which confirm the kinematics illustrated in **Figure 28a**.

It is, therefore, evident that the damage on the check rail cannot be related to the opening of the cut on the tank shell of carriage no. 1.

4.3. Initial confirmation of both wing rail and track reference stake no. 24

Figure 29 shows the digital model of the tank of carriage no. 1, obtained by reverse engineering reconstruction based on geometry acquisition with a time-of-flight laser sensor. The digital model highlights the incidence angle of the cut that varies during progressing of the cutting process. The incidence angle is the angle between the generatrix of the cylindrical body of the tank and the straight-line tangent to the outline of the cut at the point of intersection between generatrix and cut.

Figure 30 shows the photograph of the cut present on the tank shell of carriage no. 1 (**Figure 30a**) and the corresponding digital model obtained by reverse engineering reconstruction based on geometry acquisition with a time-of-flight laser sensor (**Figure 30b**).

By examining the digital models of **Figures 29** and **30b**, it can be noted that the cut starts with an incidence angle of 5.1° and ends with an incidence angle of 9.8°. Accordingly, the rotation of the tank around a vertical axis, as illustrated in **Figure 12**, was about 5°.

In **Figure 31**, the digital model of the wing rail, obtained by reverse engineering reconstruction based on geometry acquisition with a structured light optical sensor, is reported in side view (**Figure 31a**) and longitudinal view (**Figure 31b**). It can be noted that the blunted surface of

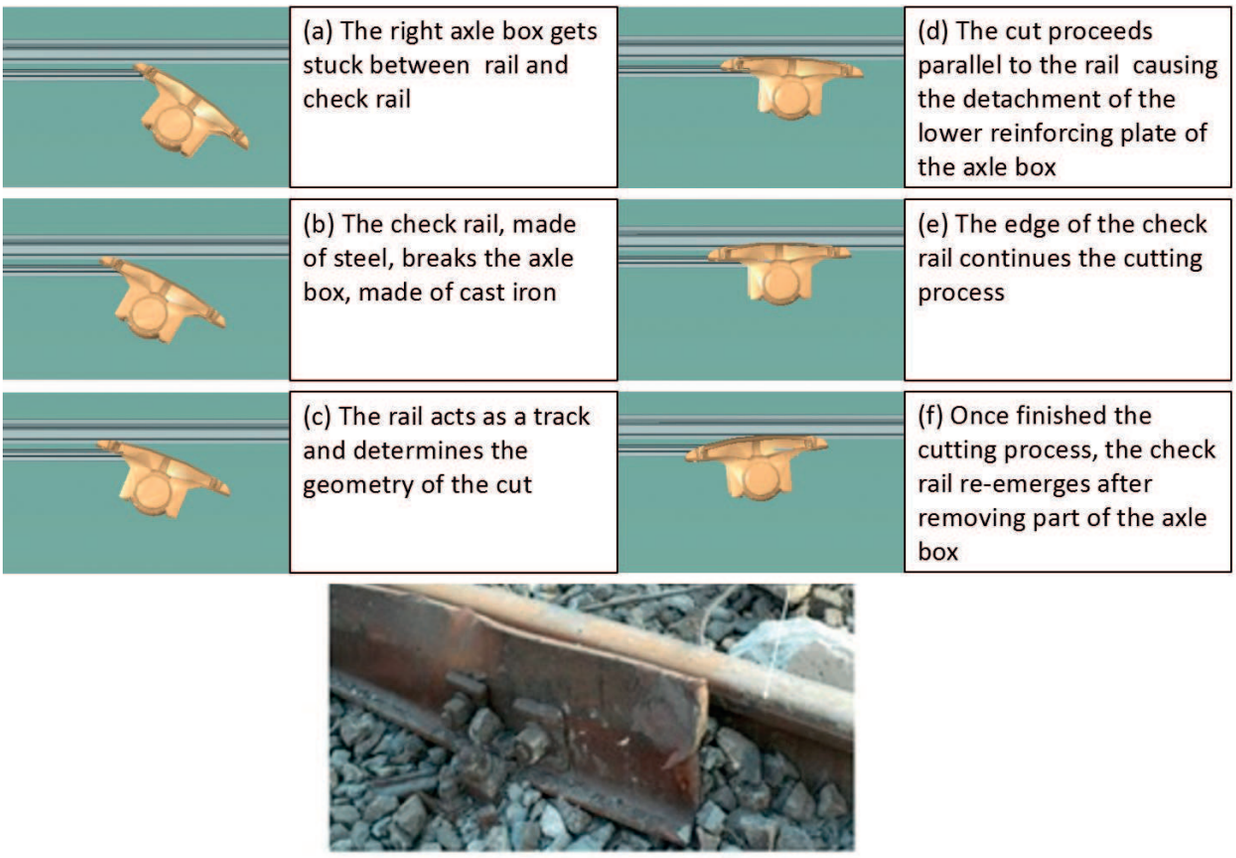

Figure 28. (a) Simulation reconstruction of the kinematics of the impact between check rail and right axel box of the first wheel set of the front bogey of carriage no. 1 and (b) traces of damage on the check rail confirming the kinematics described in **Figure 28a**.

the extremity of the wing rail interested by the damage does not evidence traces of abrasion due to sliding.

Figure 32 illustrates the simulation of the interaction between wing rail (the digital model of which was considered fixed with respect to the ground) and the deformed area of the tank

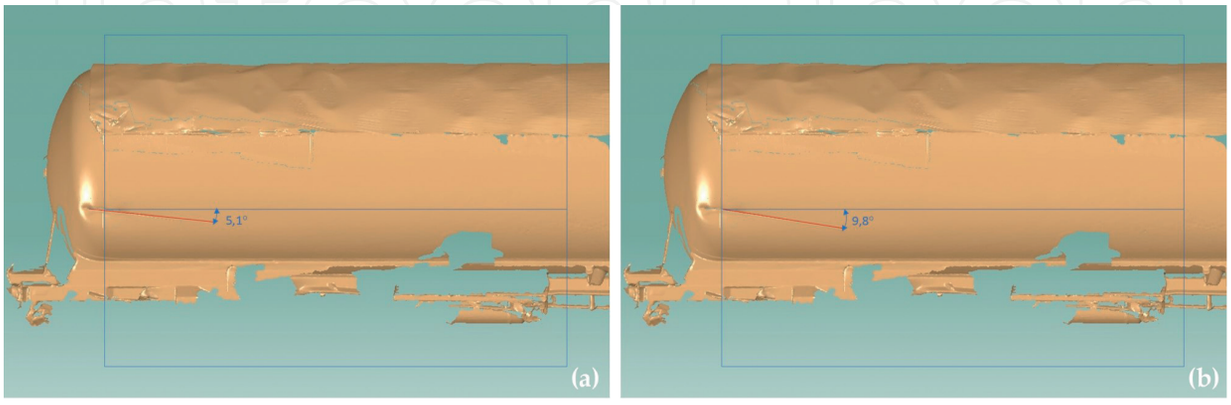

Figure 29. Digital twin of the tank of carriage no. 1. Obtained by reverse engineering reconstruction based on geometry acquisition with a time-of-flight laser sensor, with indication of the incidence angle of (a) beginning of the cut and (b) end of the cut.

http://dx.doi.org/10.5772/intechopen.73233

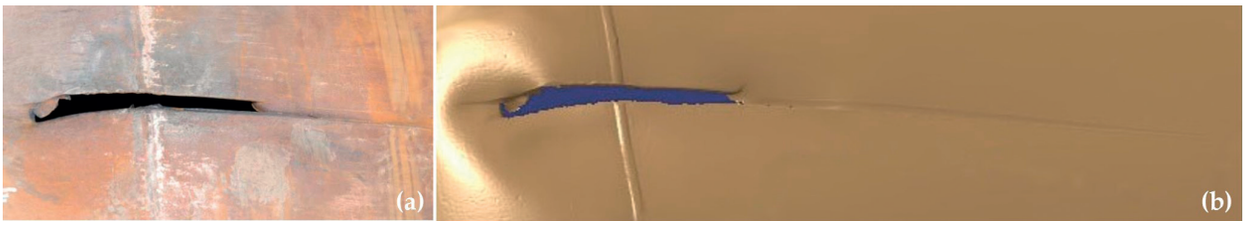

Figure 30. (a) Photograph of the cut present on the tank shell of carriage no. 1 and (b) digital model of the cut obtained by reverse engineering reconstruction based on geometry acquisition with a time-of-flight laser sensor.

shell of carriage no. 1. The simulation comprises the following phases: (a) initial contact between wing rail and shell of the tank, (b) penetration into the sheet metal of the tank shell and start of the cutting, (c) progressing of the cutting process, (d) end of the cutting, (e) start of the sliding on the tank shell surface, and (f) end of the sliding.

Figure 33a and **b** shows the details of the cutting phases corresponding to the positions of **Figure 32c** and **d**, respectively.

The analysis of the diverse relative positions of the wing rail and the cut opening shows a geometrical compatibility between the two digital models during the cutting process.

The same simulation was carried out by considering the damage caused by track reference stake no. 24, the digital model of which, realized by reverse engineering reconstruction based on geometry acquisition with a structured light optical sensor, is reported in **Figure 34**. The figure shows a view from the head side (**Figure 34a**) and from the flange side (**Figure 34b**) of the rail chunk making up the track reference stake, evidencing the highly abraded sharp corner.

Figure 35 shows the simulation of the interaction between track reference stake no. 24 and side of the tank shell of carriage no. 1, comprising the following phases: (a) initial contact between track reference stake and tank shell side, (b) penetration into the tank shell

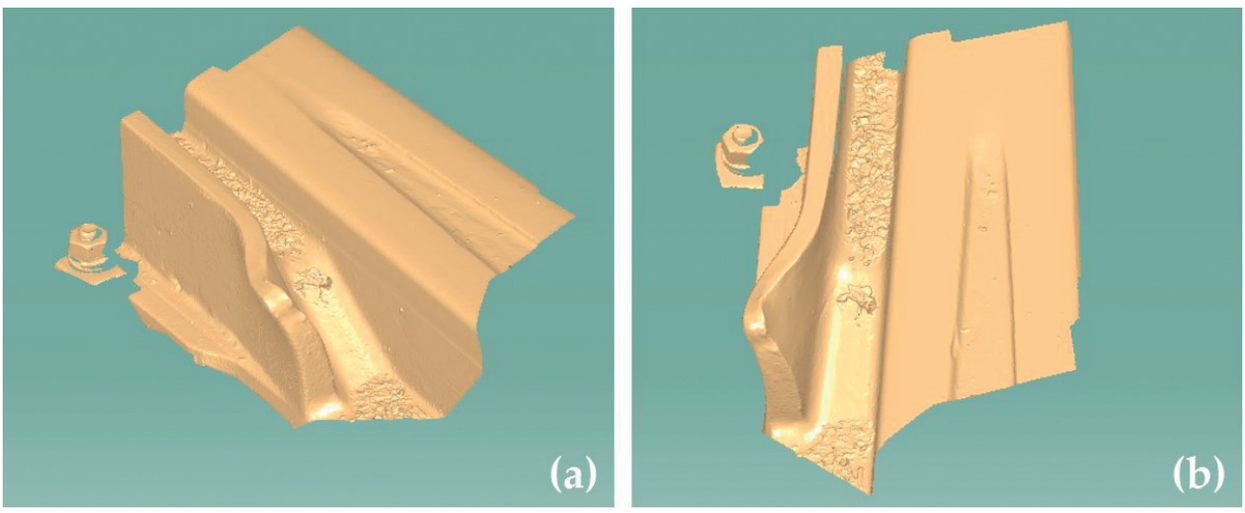

Figure 31. Digital twin of the wing rail obtained by reverse engineering reconstruction based on geometry acquisition with a structured light optical sensor: (a) side view and (b) longitudinal view.

side and start of cutting (c), (d) end of cutting, (e) start of sliding, and (f) end of sliding on the shell surface.

Figure 36a and **b** shows the details of the phases of the cutting action by track reference stake no. 24 corresponding to the positions of **Figure 35c** and **d**, respectively.

Also the analysis of this simulation confirms the geometrical compatibility between the shape of track reference stake no. 24 and the opening generated by its cutting action on the tank shell,

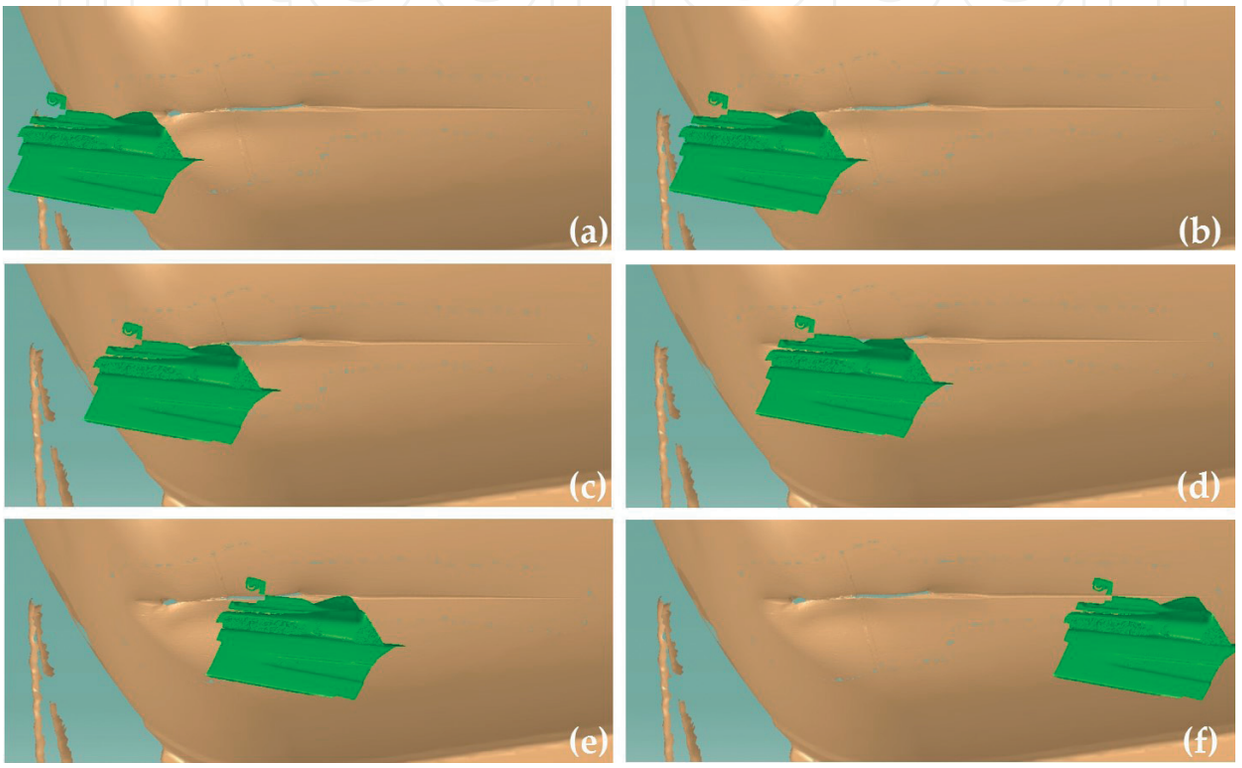

Figure 32. Simulation of the interaction between wing rail and tank shell of carriage no. 1: (a) contact, (b) penetration, (c) cutting, (d) exit, (e) start of sliding, and (f) end of sliding.

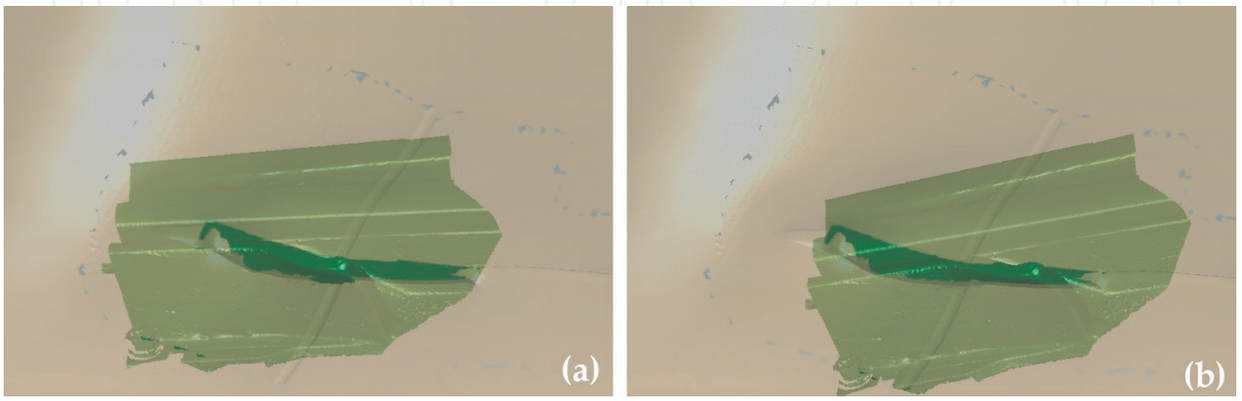

Figure 33. Details of the phases of the cutting action by the wing rail corresponding to: (a) the position of **Figure 32c** and (b) the position of **Figure 32d**.

http://dx.doi.org/10.5772/intechopen.73233

taking into account the yielding and knocking down of track reference stake no. 24 under the impact of tank carriage no. 1.

Thus, the analyses of the damage generation process, carried out by simulating the relative displacements between the deformed zone of the tank shell and the possible responsible elements encountered by carriage no. 1 during the accident, evidenced that both wing rail

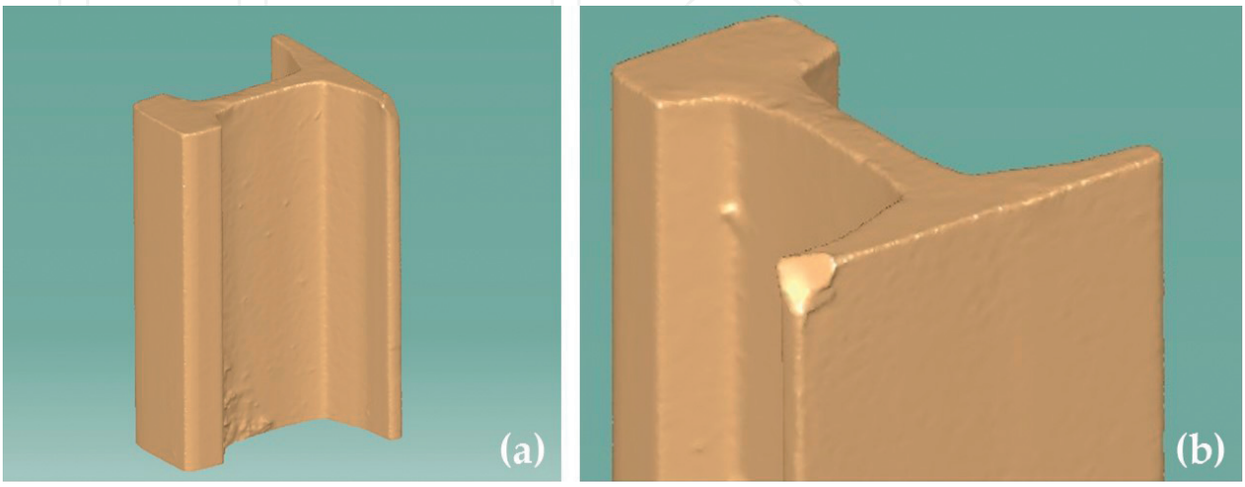

Figure 34. Digital twin of track reference stake no. 24, obtained by reverse engineering reconstruction based on geometry acquisition with a time-of-flight laser sensor: (a) view from the head side and (b) view from the flange side, evidencing the highly abraded sharp corner.

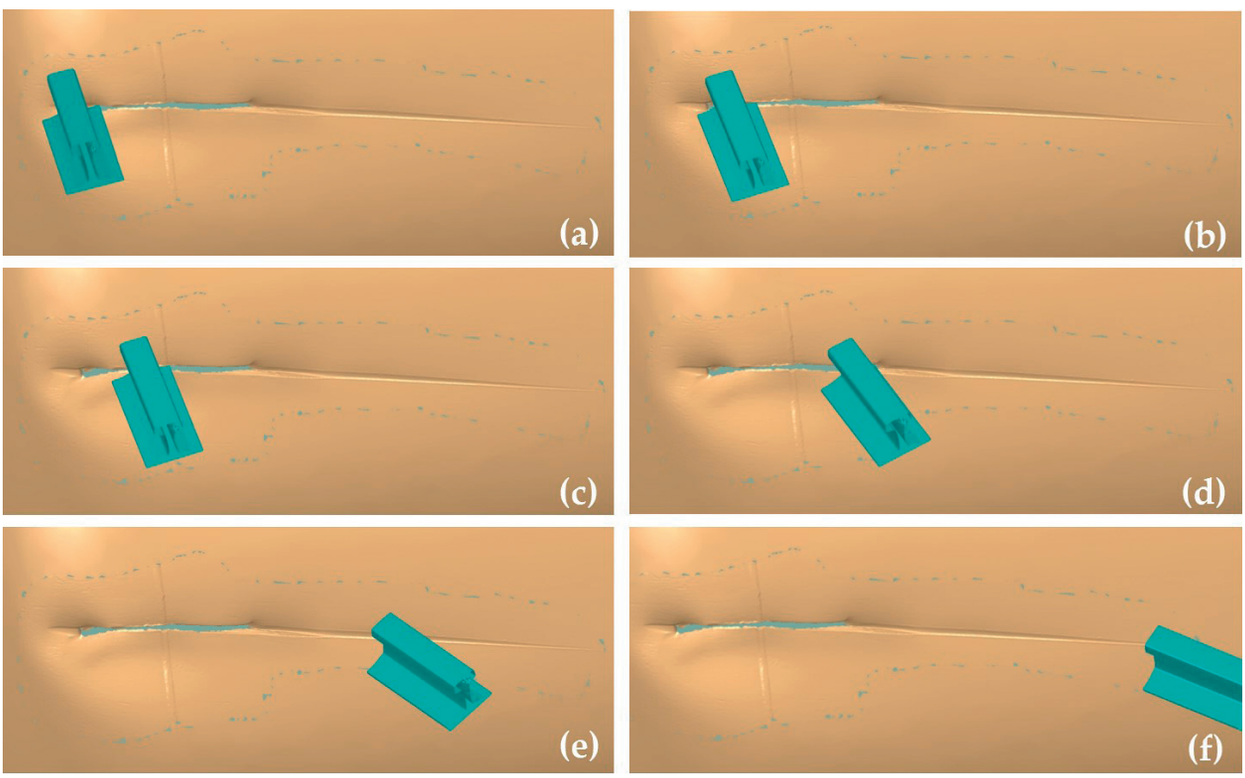

Figure 35. Simulation of the interaction between track reference stake no. 24 and tank shell side of carriage no. 1: (a) initial contact, (b) penetration, (c) start of cutting, (d) end of cutting, (e) start of sliding, and (f) end of sliding.

and track reference stake no. 24 could be geometrically compatible with the shape of the cut on the tank shell.

4.4. Wing rail final exclusion

However, the previous simulation analyses were limited to the verification, from a geometrical point of view, of the local compatibility of the elements possibly responsible for the cut opening with the shape of the cut on the tank shell, without taking into account the positions assumed by the entire tank carriage during the cut generation process.

Therefore, the simulations were newly performed by considering the complete digital models of tank carriage no. 1 (**Figure 37**).

The positions assumed by tank carriage no. 1 during its impact against the elements possibly responsible for the cut were analyzed in the framework of the railway infrastructure with particular reference to the wing rail and track reference stake no. 24 (**Figure 38a** and **b**).

Under the hypothesis of tank shell cutting by the wing rail, **Figure 39** shows diverse visualizations of the positions assumed by the tank carriage no. 1 during the cutting phases corresponding to **Figure 32c** and **33a**.

Figure 40 shows the views of the positions assumed by tank carriage no. 1 under the hypothesis of tank shell cutting by the wing rail corresponding to **Figures 32d** and **33b**.

This simulation evidences a macroscopic interference between tank carriage no. 1 and the railway infrastructure that looks particularly evident in the more advanced phase of the cutting process, where the overlap between the tank carriage and the railway infrastructure is clearly visible (**Figure 40**).

Accordingly, even if from a geometrical point of view, the interaction between wing rail and tank shell is locally compatible with the cut shape, the carriage, in order to allow for the generation of the entire cut opening, should have assumed positions that are not compatible with the railway infrastructure. Furthermore, it must be considered that the final phase of the cutting process, consisting in the sliding of **Figure 32d**, was determined on the tank shell by an

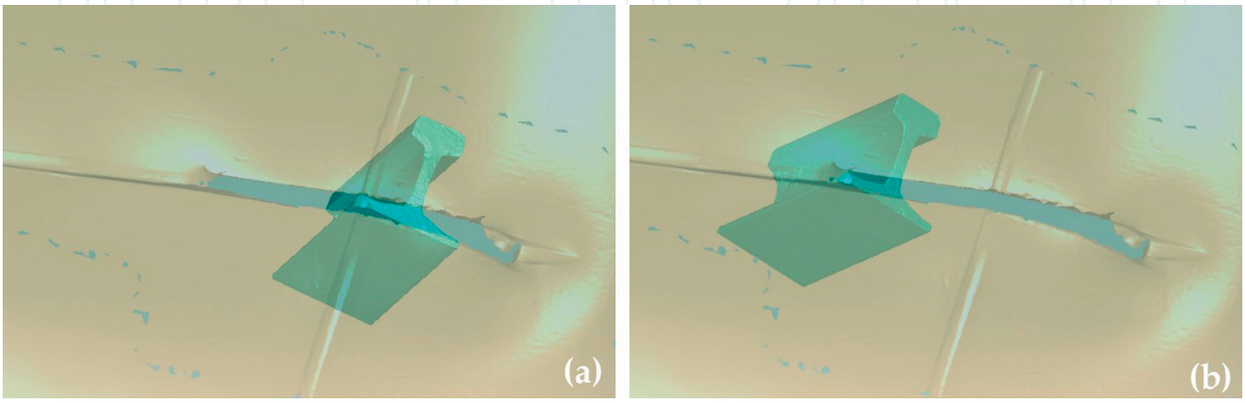

Figure 36. Details of the phases of the cutting action by track reference stake no. 24 corresponding to the position of (a) **Figure 35c** and (b) **Figure 35d**.

http://dx.doi.org/10.5772/intechopen.73233

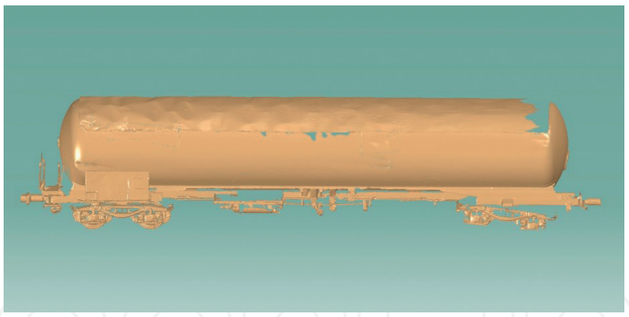

Figure 37. Digital model reconstruction of the entire tank carriage no. 1.

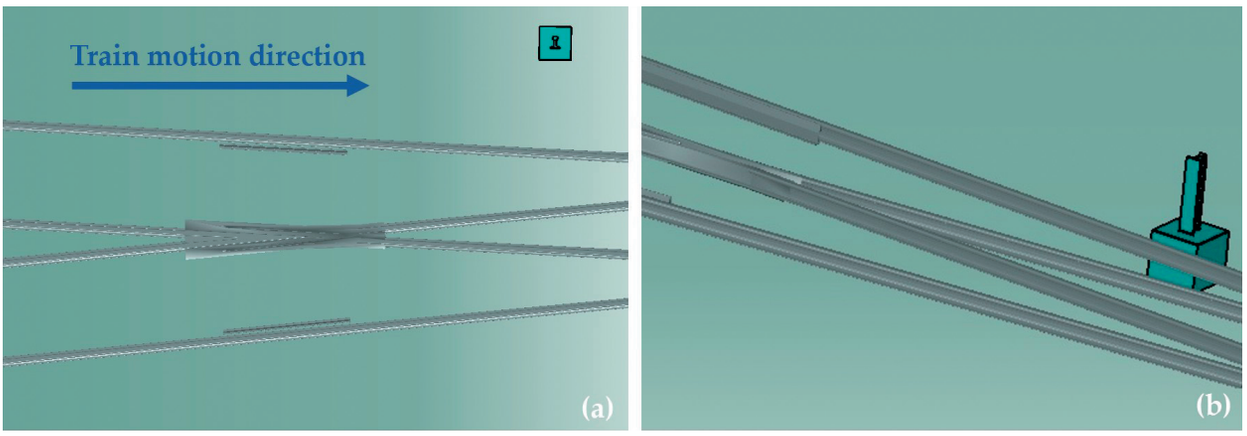

Figure 38. Digital model reconstruction of the railway infrastructure based on the planimetric measurements of the accident scene: (a) position of the wing rail and (b) lateral view of the position of track reference stake no. 24.

object with a sharpened corner shape and not with a blunted corner shape such as the one of the wing rail (**Figure 31**).

It can thus be stated that the wing rail cannot have been the cause of the cut opening on the tank shell side.

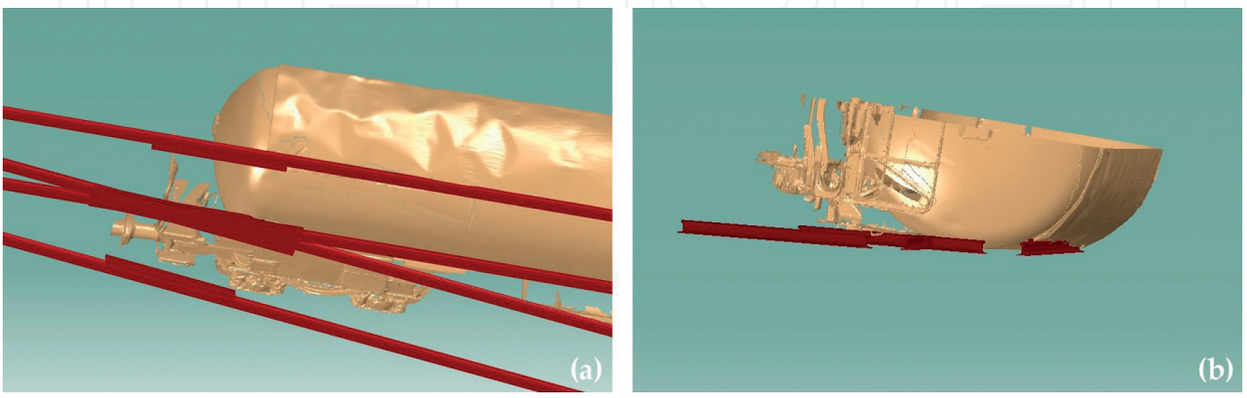

Figure 39. Views of the positions assumed by tank carriage no. 1 in the framework of the railway infrastructure under the hypothesis of tank shell cutting by the wing rail during the phase corresponding to **Figure 32c** and **33a**.

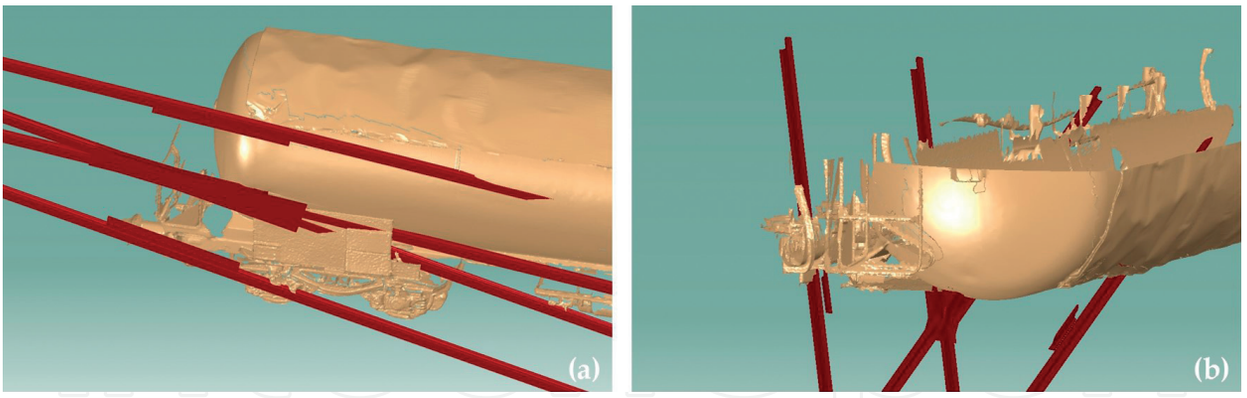

Figure 40. Views of the positions assumed by tank carriage no. 1 in the framework of the railway infrastructure under the hypothesis of tank shell cutting by the wing rail during the phase corresponding to **Figure 32d** and **33b**.

4.5. Track reference stake no. 24 final confirmation

Figures 41-44 show the positions assumed by tank carriage no. 1 under the hypothesis of impact against track reference stake no. 24. In particular, the results refer to the following phases of the cutting process: initial contact (**Figures 35a** and **41**, penetration (**Figures 35b** and **42**), cutting (**Figures 35c** and **43**), and sliding (**Figures 35d** and **44**). The simulations took into account the yielding of track reference stake no. 24, which under the impact action by the tank vessel, was tilted till it knocked down sideways (**Figure 35**).

The simulation results show that, under the hypothesis of tank shell cutting by track reference stake no. 24, no interference is evidenced between tank carriage no. 1 and the railway infrastructure during the tank shell cutting process.

Accordingly, the tank of carriage no. 1, already overturned on its left side, impacted with its front part against track reference stake no. 24, which started the cutting action by penetrating for a certain depth inside the tank shell and continued to cut the sheet metal of the tank shell till it exited from the cut opening after its knocking upon yielding of the ballast where it was grounded.

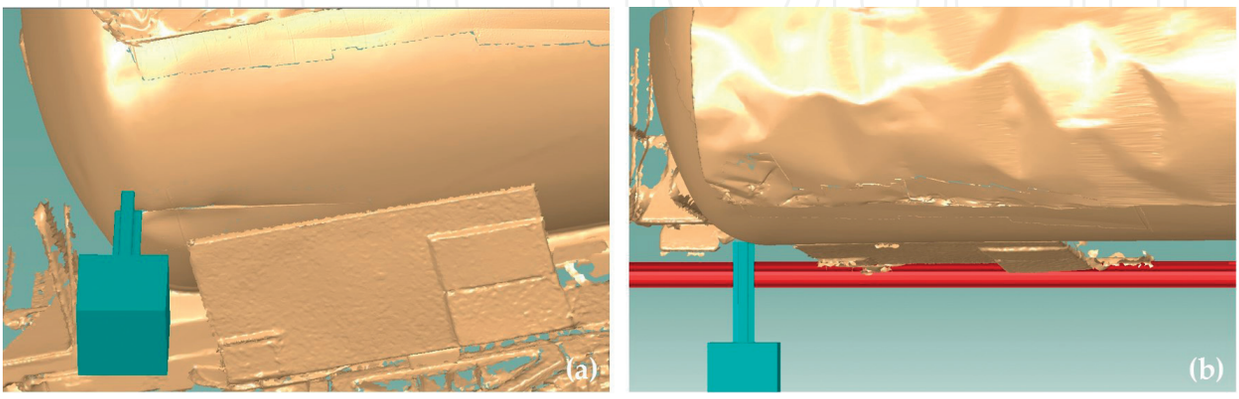

Figure 41. Position assumed by tank carriage no. 1 in the framework of the railway infrastructure under the hypothesis of tank shell cutting by track reference stake no. 24: initial contact phase (**Figure 35a**).

http://dx.doi.org/10.5772/intechopen.73233

Figure 45a and **b** shows the details of the position of track reference stake no. 24 during the penetration phase into the tank shell.

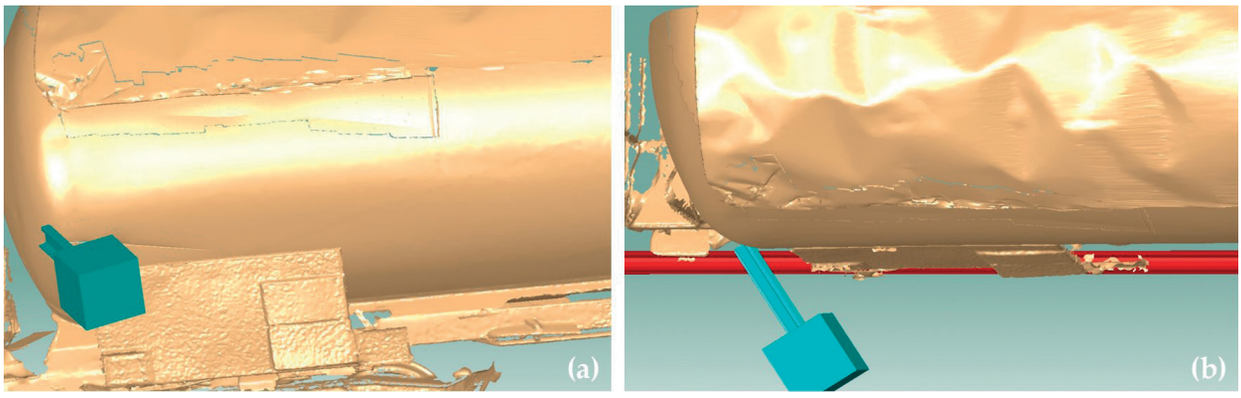

Figure 42. Position assumed by tank carriage no. 1 in the framework of the railway infrastructure under the hypothesis of tank shell cutting by track reference stake no. 24: penetration phase (**Figure 35b**).

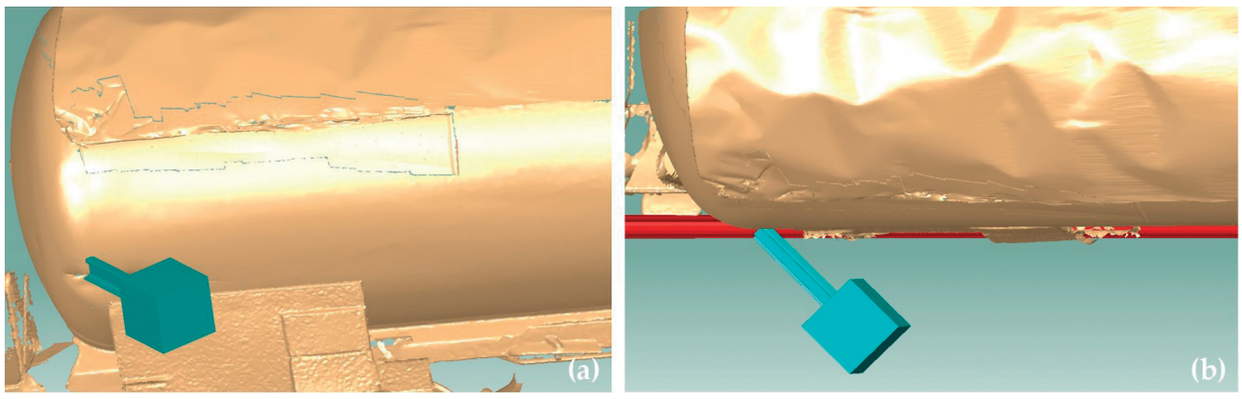

Figure 43. Position assumed by tank carriage no. 1 in the framework of the railway infrastructure under the hypothesis of tank shell cutting by track reference stake no. 24: cutting phase (**Figure 35c**).

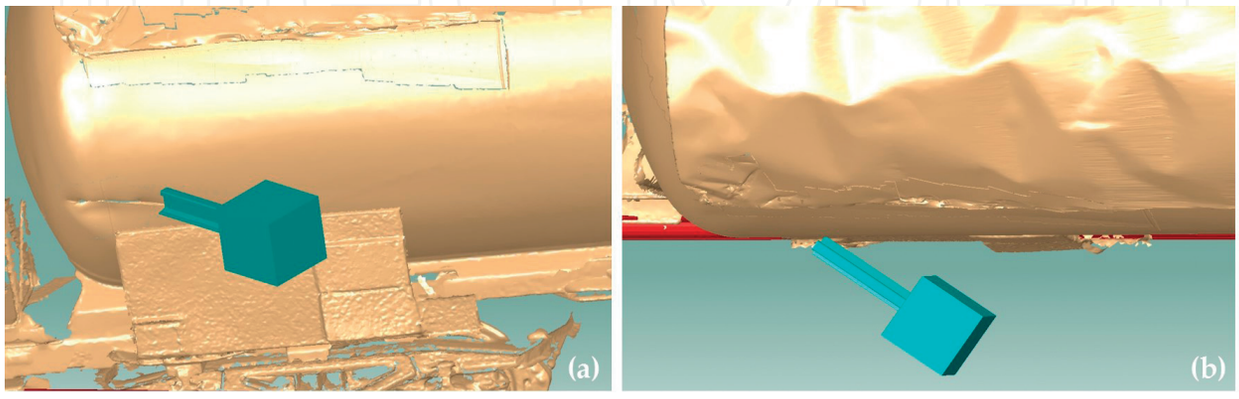

Figure 44. Position assumed by tank carriage no. 1 in the framework of the railway infrastructure under the hypothesis of tank shell cutting by track reference stake no. 24: sliding phase (**Figure 35d**).

During the last phase of interaction, track reference stake no. 24, reversed on the track ballast, could not continue its cutting action on the sheet metal of the tank shell; however, it stuck out of the ground enough to be able to mark the tank shell with a long scratch starting from the end of the cut opening. During this final phase, the sliding between tank shell and track reference stake no. 24 determined the abrasion of the sharp edge of the stake, as evidenced in **Figure 37**. **Figure 46** shows diverse views of the position of track reference stake no. 24 during the final sliding phase against the tank shell.

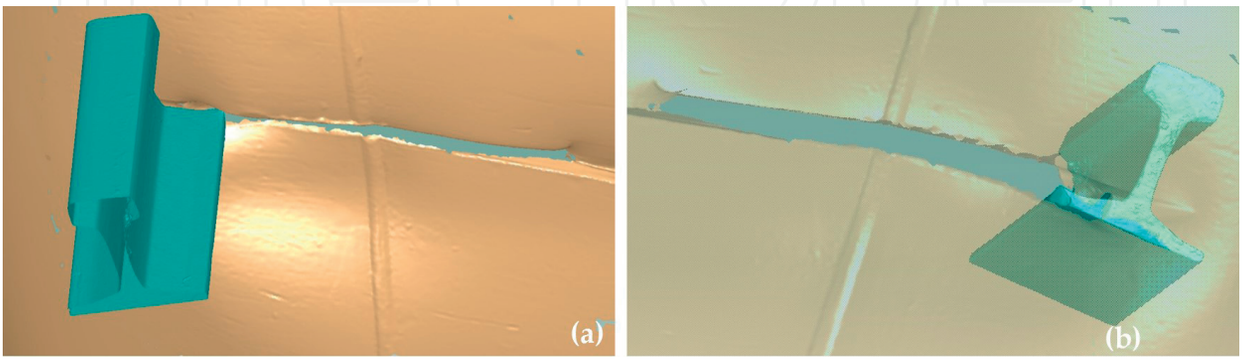

Figure 45. Details of the position of track reference stake no. 24 during the penetration phase into the tank shell: (a) view from the outside of the tank and (b) view from the inside of the tank.

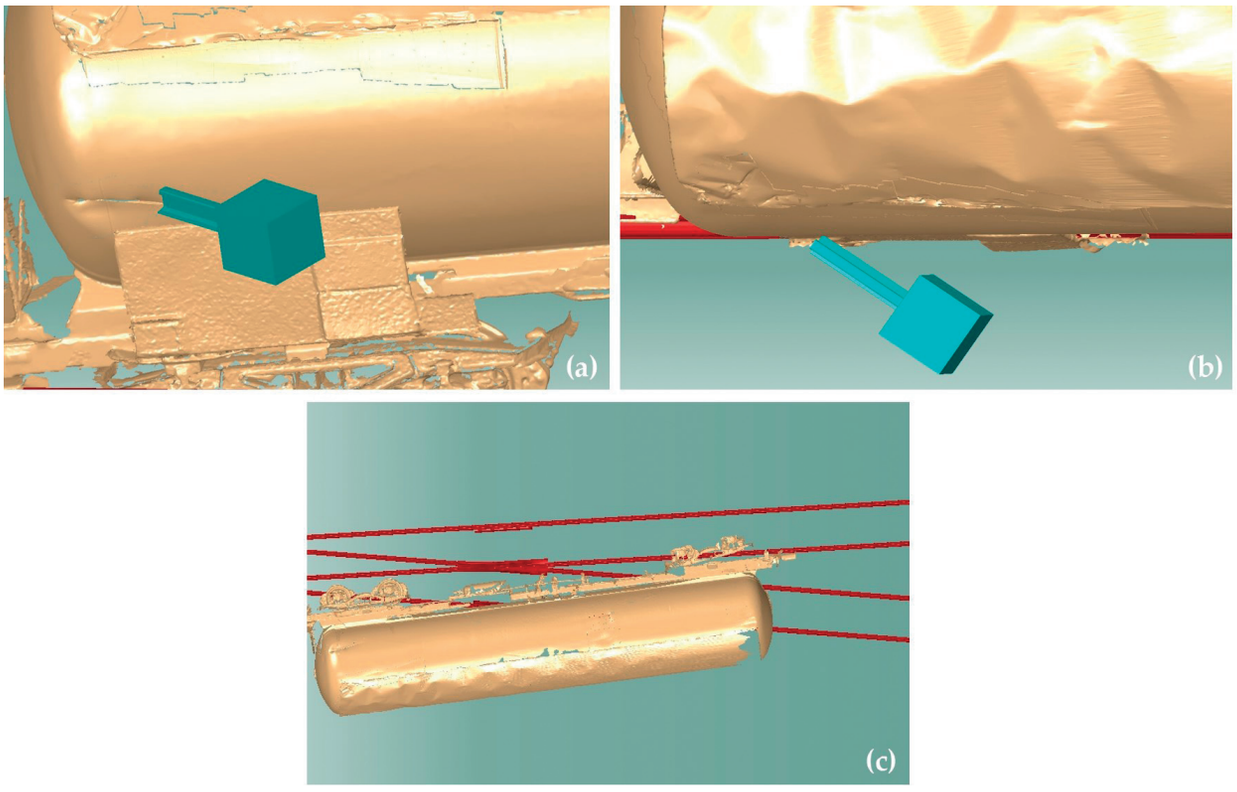

Figure 46. Position of track reference stake no. 24 during the sliding phase against the tank shell.

http://dx.doi.org/10.5772/intechopen.73233

It can thus be stated that the track reference stake has been the actual cause of the cut opening on the tank shell side.

5. Conclusions

With reference to a real catastrophic train accident where a railway tank carriage, carrying a pressure vessel filled with liquefied petroleum gas, collided with an obstacle that generated a cut in the tank shell, causing a gas leakage with consequent explosion and fire responsible for a high number of human casualties, traditional railway accident reconstruction procedures identified two potential objects accountable for the cutting of the pressure vessel shell—a wing rail and a track reference stake.

In this work, based on digital terrain models and reconstructed models of the railway carriage and the objects possibly responsible for the cut damage on the tank shell, 3D digital simulation scenarios were created, allowing to position and rotate the carriage interactively to detect every possible collision of the pressure vessel with the infrastructure environment. The scope was to investigate whether the form of the cut in the pressure vessel fits to the damage found on the objects potentially accountable for the cutting of the tank shell and whether the interference between object and shell could generate the resulting metal chip, found in the tank, through an interaction similar to a metal cutting operation.

The digital simulation of the developments of the collision between railway tank carriage and infrastructure allowed to observe the potential carriage displacements during the accident from any angular viewpoint. The interference related to collisions between railway tank carriage and the objects in the infrastructure environment potentially responsible for the cut opening was highlighted, allowing to identify the most likely root cause of the catastrophic railway accident.

The analyses of the cut damage process carried out by simulating the relative displacements between the deformed zone of the tank shell and the objects possibly responsible for the cut provided the evidence that two such objects, i.e., a wing rail and a track reference stake, could be geometrically compatible with the shape of the cut.

However, the analyses were limited to the verification, from a geometrical point of view, of the local compatibility between each object and the shape of the cut shape on the tank shell, without taking into account the positions assumed by the entire tank carriage during the cut generation process.

Thus, the simulations were newly performed by considering the complete digital models of the railway tank carriage. The positions assumed by this tank carriage during the simulated impact against the objects possibly responsible for the cut were analyzed with particular reference to the wing rail and the track reference stake in the infrastructure environment.

Under the hypothesis of cut damage determined by the wing rail, the simulation of the positions assumed by the tank carriage during the cutting phases evidences a macroscopic interference between tank carriage and the railway infrastructure that looks particularly

evident in the more advanced phase of the cut opening process, where the overlap between the tank carriage and the railway infrastructure is clearly visible.

Accordingly, even if from a geometrical point of view, the interaction between wing rail and tank shell is locally compatible with the cut shape, the carriage, in order to allow for the generation of the entire cut opening, should assume positions that are not compatible with the railway infrastructure. Furthermore, it must be considered that the final phase of the cutting process, consisting in the sliding against the pressure vessel shell, was determined on the tank shell side by an object with a sharpened corner shape and not with a blunted corner shape such as the one of the wing rail. It can thus be stated that the wing rail cannot have been the cause of the cut opening on the tank shell.

Under the hypothesis of cutting caused by the track reference stake, the simulations of the positions assumed by the railway tank carriage during the cutting phases show that no interference is established between tank carriage and the railway infrastructure during the cut opening process of the tank shell.

Accordingly, the tank of the railway carriage, already overturned on its left side, impacted with its front part against the track reference stake. The latter started the cutting action by penetrating for a certain depth inside the tank shell and continued to cut the sheet metal of the tank shell till it exited from the cut opening as it knocked down upon being removed from the ballast where it was grounded.

During the last phase of interaction, the track reference stake, reversed on the track ballast, could not continue its cutting action on the sheet metal of the tank shell; however, it stuck out of the ground enough to be able to mark the tank shell with a long scratch starting from the end of the cut opening. During this final phase, the sliding between tank shell and track reference stake determined the abrasion of the sharp edge of the stake. It can thus be maintained that the track reference stake has been the actual cause of the cut opening on the tank shell side.

As described in Section 3.1, the traditional system for railway track curve geometry periodic checking is based on the installation of reference stakes made of rail chunks grounded in the ballast every 10 m next to the track curve to be checked and protruding vertically out of the ground level. This practice poses a major hazard due to the presence of permanently installed vertical rail chunks characterized by sharp corners that, in case of impact against rail carriages for transportation of dangerous goods or of passengers, can cause considerable damage or even provoke catastrophic events.

The introduction of alternative track positioning and control systems, capable to provide more advanced solutions for safer conditions in the railway infrastructure and operations, is highly desirable to avoid future disastrous accidents of the kind reported in this work. One such alternative system is represented by the railway surveying system already introduced by the national railways in Germany and Norway [12]. Its operation requires the setting, along the track of interest, of topographic reference points, the position of which is previously determined through a precision polygon. Through traditional topographic methods, these points are subsequently referred to by the points materialized through fastening devices, incorporated in the concrete basis of the poles or portals of the electric power line, for the positioning

of the measuring instrument. A main advantage of this alternative system over the traditional track positioning and control system is that the track axis is referred to an absolute coordinate system, which allows for the "free" positioning of the measurement station outside the influence of the train movement, without interference with the railway operation. A further major advantage is that there is no more need for track reference stakes: this notably reduces the installation costs, due to the much smaller number of low cost reference points, as well as the complete elimination of sharp corner rail chunks permanently standing in the railway infrastructure, thus providing a vital improvement in the railway operational safety.

Author details

Alessandra Caggiano[1,2]* and Roberto Teti[1,3]

*Address all correspondence to: alessandra.caggiano@unina.it

1 Fraunhofer Joint Laboratory of Excellence on Advanced Production Technology (Fh-J_LEAPT UniNaples), Naples, Italy

2 Department of Industrial Engineering, University of Naples Federico II, Naples, Italy

3 Department of Chemical, Materials and Industrial Production Engineering, University of Naples Federico II, Naples, Italy

References

[1] Ministero delle Infrastrutture e Trasporti. Relazione d'indagine sull'incidente ferroviario di Viareggio. 2 aprile 2014. 84 p

[2] Chandra S. Railway Engineering. India: Oxford University Press, Inc.; 2008

[3] Mundrey JS. Railway Track Engineering. India: Tata McGraw-Hill Education. 2009

[4] Bonnet CF. Practical Railway Engineering. UK: Imperial College Press; 2005

[5] Toni P. Ricostruzione della dinamica dell'incidente ed individuazione delle cause che lo provocarono. Consulenza tecnica di ufficio, Procura della Repubblica presso il Tribunale di Lucca, Italy; 2011

[6] Teti, R. Relazione tecnica di parte: Ricostruzione della dinamica dell'incidente ferroviario di Viareggio del 29.06.2009 e individuazione delle cause del disastro. 2012

[7] Caggiano A, Nele L, Sarno E, Teti R. 3D digital reconfiguration of an automated welding system for a railway manufacturing application. Procedia CIRP. 2014;**25**:39-45

[8] Raja V, Fernandes KJ, editors. Reverse Engineering: An Industrial Perspective. London: Springer-Verlag; 2008. 242 p

[9] Bernard A. Virtual engineering: Methods and tools. Journal of Engineering Manufacture. 2005;**219**(B5):413-422

[10] Barone S, Razionale AV. Relazione tecnica rilievi 3D ed analisi delle condizioni geometriche di danneggiamento del carro cisterna 3380 781 8 210-6 del treno 50325 a seguito dello svio del 29/06/2009. Pisa. 21/10/2010

[11] Segreto T, Caggiano A, D'Addona DM. Assessment of laser-based reverse engineering systems for tangible cultural heritage conservation. International Journal of Computer Integrated Manufacturing. 2013;**26**(9):857-865

[12] Aquilino E, Colonna P, Tragni O. Le innovazioni tecnologiche nei metodi di tracciamento e controllo delle curve ferroviarie. In: Convegno SIIV. (Società italiana di infrastrutture viarie); Cagliari. 1999. pp. 1-18